BIOCHEMISTRY
including biophysical chemistry & molecular biology

Article

pubs.acs.org/biochemistry

Molecular Hairpin: A Possible Model for Inhibition of Tau Aggregation by Tannic Acid

Junliang Yao,[†] Xing Gao,[†] Wenliang Sun,[†] Tianming Yao,*[,†] Shuo Shi,*[,†] and Liangnian Ji[‡]

[†]Department of Chemistry, Tongji University, Shanghai 200092, China

[‡]MOE Laboratory of Bioinorganic and Synthetic Chemistry, School of Chemistry and Chemical Engineering, Sun Yat-Sen University, Guangzhou, China

ABSTRACT: Inhibition of anomalous aggregation of tau protein would be an attractive therapeutic target for Alzheimer's disease (AD). In this study, tannic acid (TA), a polymeric plant polyphenol, and its monomer, gallic acid (GA), were introduced as the references to afford a molecular framework that integrates tau binding properties and inhibitory effects. Using a thioflavin S fluorescence assay and electron microscopy, we demonstrated that TA could competently inhibit the in vitro aggregation of tau peptide R3, corresponding to the third repeat unit of the microtubule-binding domain, with an IC_{50} of 3.5 μM, while GA's inhibition was comparatively piddling (with an IC_{50} of 92 μM). In the isothermal titration calorimetry experiment, we found that TA could strongly bind to R3 with a large amount of heat released. Circular dichroism spectra showed TA dose-dependently suppressed the conformational transition of R3 from a random coil structure to a β-sheet structure during the aggregation process. Finally, a structural model was built using molecular docking simulation to elucidate the possible binding sites for TA on the tau peptide surface. Our results suggest that TA recognizably interacts with tau peptide by forming a hairpin binding motif, a key framework required for inhibiting tau polymerization, in addition to hydrogen bonding, hydrophilic−hydrophobic interactions, and static electrical interactions, as reported previously. The inhibitory effect of TA on human full-length tau protein (tau_{441}) was also verified by electron microscopy. This finding hints at the possibility of TA as a leading compound of anti-AD drugs and offers a new stratagem for the rational molecular design of a tau aggregation inhibitor.

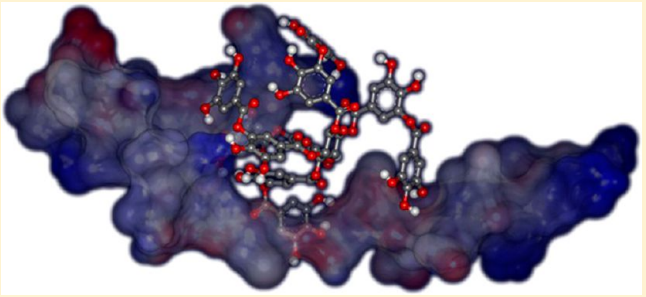

Alzheimer's disease (AD) is characterized by two hallmarks: intracellular neurofibrillary tangles (NFTs) composed of bundles of abnormally aggregated tau protein and extracellular senile plaques (SPs) consisting largely of β-amyloid (Aβ) protein.[1−3] Although the neurodegenerative processes in AD are unclear, it has in general been believed that oligomeric nucleating cores are formed initially, followed by a period of quick fibril growth during fibril formation.[4,5] Interestingly, it has been seen that the degree of cognitive impairment in AD correlates better with NFTs than with SPs.[6] Tau oligomers and paired helical filaments (PHFs) are recognized as major elements that confer cellular toxicity.[7−10]

The past decade has witnessed a renaissance of interest in inhibitors of tau aggregation as potential disease-modifying drugs for AD. Numerous small-molecule inhibitors with their ability to inhibit the assembly of tau have been described.[11−15] Reviews have summarized the available data concerning small-molecule inhibitors of tau aggregation from a medicinal chemistry point of view.[16−18] However, only a few of them have been studied for their structure−activity relationships (SARs).[11,19] Precise atomic-level structural information about the early aggregation intermediates and their small-molecule binding partners is lacking, as is a basic understanding of the fibril self-assembly processes.

Compared with β-amyloid, the lack of aromatic residues on the tau peptide chain limits its potential for hydrophobic interactions with inhibitors. Instead, hydrogen bonding or hydrophilicity has been shown to play a crucial role for tau aggregation inhibitors.[20] Phenolic hydroxyl groups are known for their greater acidity compared to that of aliphatic hydroxyl groups and for their ability to form hydrogen bonds. Hence, a group of plant polyphenols, categorized according to their structure in flavonoids, tannic acid, and lignin, have been reported to show inhibitory activity upon protein aggregation.[21,22]

We have previously performed an initial screening to correlate the number and position of the hydroxyl groups on the flavonoid moiety with inhibitory activity.[23] Another important plant polyphenol molecule in which we are most interested is tannic acid, a water-soluble ester polymerized by gallic acid. It has been demonstrated that tannic acid significantly inhibits the aggregation of Aβ.[24,25] However, very little is known about the interaction between TA and tau protein.

Received: August 6, 2012
Published: February 26, 2013

ACS Publications © 2013 American Chemical Society

dx.doi.org/10.1021/bi400240c | *Biochemistry* 2013, 52, 1893−1902

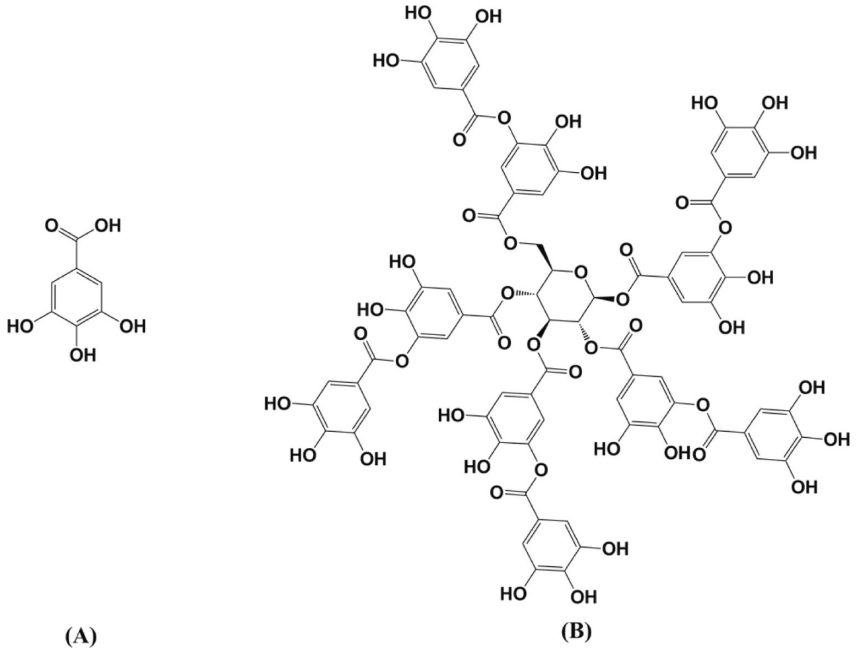

Figure 1. Chemical structures of gallic acid (A) and tannic acid (B).

This study was launched to investigate the inhibitory activity of tannic acid to tau aggregation at the atomic level, by using model protein, a short tau peptide, R3 (residues 306−336, VQIVY KPVDL SKVTS KCGSL GNIHH KPGGG Q, according to the longest tau peptide), corresponding to the third repeat unit of the microtubule-binding domain of tau. R3 is believed to be pivotal for the biochemical properties of full tau protein, because (1) R3 forms the core of PHFs produced during tau aggregation,[26] (2) R3 exhibits the highest self-assembly speed and the lowest critical concentration in filament formation,[27] and (3) the tau aggregation process is believed to be initiated from the VQIVYK hexapeptide ($tau_{306-311}$), which is located at the N-terminus of R3.[28] All our experiments were conducted using a polymeric plant polyphenol, tannic acid, in comparison with its molecular monomer, gallic acid (Figure 1). We demonstrated that TA could competently inhibit R3 aggregation in vitro, while GA's inhibition was comparatively piddling. We found that TA could strongly bind to R3 with a large amount of heat released. Meanwhile, TA dose-dependently suppressed the conformational transition of R3 from a random coil structure to a β-sheet structure during the aggregation process. Finally, using molecular simulation, a structural model was built to elucidate the possible docking orientation for TA on the tau peptide surface. Our results suggest that tau peptide recognizably interacts with TA by forming a hairpin structure, a key structural feature required for inhibiting tau polymerization, in addition to hydrogen bonding, hydrophilic−hydrophobic interaction, and static electrical interaction, as reported previously.[18] The inhibition of human full-length tau by TA was also verified by electron microscopy. This finding hints about the possibility of TA as a leading compound of anti-AD drugs and offers a new stratagem for the rational molecular design of a tau aggregation inhibitor.

MATERIALS AND METHODS

Materials. The R3 peptide was synthesized using a solid-phase peptide synthesizer and purified by reverse-phase high-performance liquid chromatography (HPLC) to a 95.0% level. The purified peptide was lyophilized and stored at −20 °C before it was used. A fresh working solution of R3 was prepared in Tris-HCl buffer (50 mM, pH 7.5) with a peptide concentration of 1 mg/mL. The 441-amino acid isoform of human brain tau was purchased from Sigma-Aldrich (T0576, tau_{441} human). Heparin (average molecular weight of 6000) and ThS were also purchased from Sigma-Aldrich. Tannic acid and the other chemicals were of analytical reagent grade. All the experiments were conducted under an open atmosphere.

Kinetics of R3 Aggregation and Inhibition Monitored by Fluorescence. The fluorescence experiments were performed on a Hitachi F-7000 fluorescence spectrophotometer with a 2 mm quartz cell maintained at 37 °C using a circulating water bath. A 15 μM solution of R3 was prepared using 50 mM Tris-HCl buffer (pH 7.5), and 10 μM thioflavin S (ThS) dye was added to the R3 solution prior to the determination. Aggregation was induced by the addition of heparin (final concentration of 3.8 μM). For the inhibition assay, 7.5, 15, and 30 μM tannic acid were added to the reaction mixture, and the kinetics of each sample was immediately monitored with a fluorescence spectrophotometer, with excitation at 440 nm and emission at 500 nm. The excitation and emission slit widths were both set at 10 nm. For each curve of time-dependent ThS fluorescence, the measurement was taken three times and averaged. The background fluorescence of the sample was removed when necessary. The inhibition of R3 aggregation by gallic acid was also investigated following the method discussed above for comparison.

IC_{50} Determination. A 1 mg/mL stock solution of R3 was diluted to a final concentration of 15 μM in 500 μL of Tris-HCl buffer containing 3.8 μM heparin, in the absence or presence of TA or GA at different concentrations (0−15 μM for TA and 0−150 μM for GA), and incubated at 37 °C for 4 h. Then ThS (final concentration of 10 μM) was added to each solution, and fluorimetry was performed using a Hitachi F-7000 fluorescence spectrophotometer (excitation at 440 nm and emission at 500 nm). The IC_{50} value was calculated for each compound.

dx.doi.org/10.1021/bi400240c | *Biochemistry* 2013, 52, 1893−1902

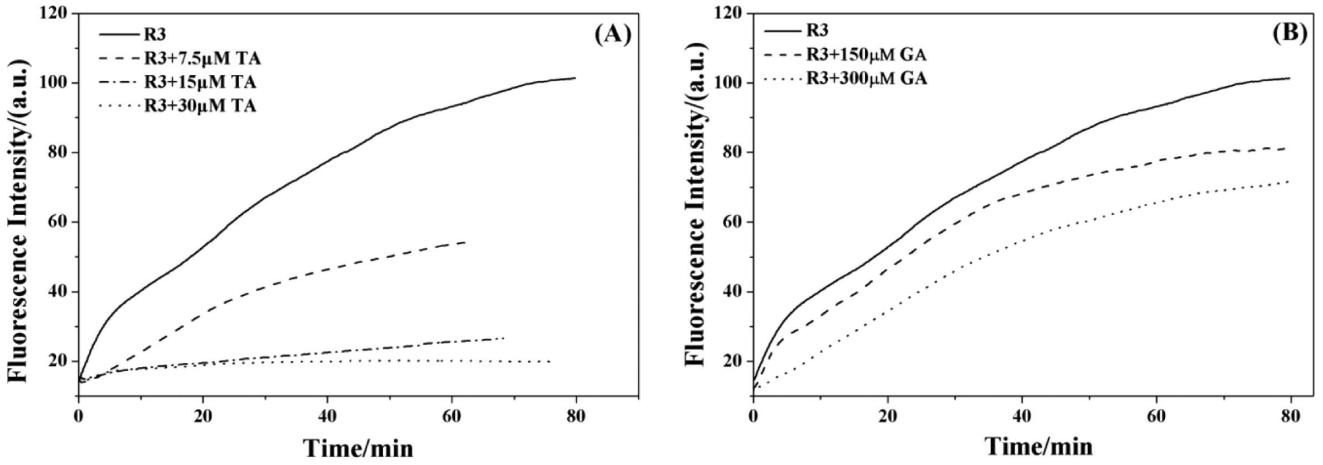

Figure 2. Effects of TA and GA on the kinetics of R3 aggregation. (A) Aggregation of 15 μM R3 in the absence and presence of 7.5, 15, and 30 μM TA. (B) Aggregation of 15 μM R3 in the absence and presence of 150 and 300 μM GA.

Inhibition of Peptide Oligomers. The diluted R3 samples (15 μM) in a 50 mM Tris-HCl buffer solution (pH 7.5) containing 3.8 μM heparin and 10 μM ThS were incubated at 37 °C for 5, 10, 20, 30, 40, 50, and 60 min. Each of the resulting solutions contained a certain portion of oligomers different from the others' because of the discrepancy of the incubation time. The fluorescence of each sample was recorded on a Hitachi F-7000 fluorescence spectrophotometer (λ_{ex} = 440 nm; Exslit = Emslit = 10 nm) with a 2 mm quartz cell maintained at 37 °C using a circulating water bath. A fixed amount of TA (15 μM) was then added to each sample, and the mixed solutions were further incubated for 2 h, following a fluorescence characterization. The fluorescence intensities at 500 nm were collected to examine the impact of TA on the oligomers of tau peptide during the early aggregation process.

CD Measurement. The sample solutions of R3 (15 μM) were prepared using 20 mM phosphate buffer (pH 7.5) in the absence or presence of TA, and an optimal concentration of heparin (3.8 μM) was added to induce the aggregation of each reaction mixture. All measurements were taken at 37 °C with a JASCO J-810 spectrometer under a constant flow of nitrogen gas. A cuvette with a 10 mm path length was used for spectra recorded between 190 and 260 nm with sampling points every 0.1 nm. The measurement for each experiment was repeated three times, and the results were collected. Direct data of each sample (θ, in millidegrees) were converted to mean residue ellipticity ($[\theta]$ in degrees square centimeters per decimole) using the equation $[\theta] = \theta/(cl)$, where c is the concentration (15 μM) and l is the path length (10 mm).

EM Measurement. *Characterization of the R3 Filament Morphology.* The reaction mixtures containing 15 μM R3 and 3.8 μM heparin were prepared with 50 μM Tris-HCl buffer (pH 7.50) in the absence or presence of TA (0, 3, or 15 μM). The solutions were then incubated at 37 °C for 4 h. After that, reaction mixtures were spread on 600-mesh copper grids, negatively stained with 2% uranyl acetate, and examined under an electron microscope (JEOL JSM-1200EX II) with an acceleration voltage of 80 kV.

Semiquantitative Assessment of TA's Inhibition on Filament Formation of Full-Length Tau. The full-length tau (1.0 mg/mL) and heparin (0.10 mg/mL) were incubated at 37 °C for 72 h in 50 μL of 50 mM Tris-HCl (pH 7.5) containing 0.1% sodium azide as described previously,[21] in the presence or absence of tannic acid (0, 30, or 60 μM). Aliquots (5 μL) of assembly mixtures were placed on collodion-coated 600-mesh copper grids and stained with 2% uranyl acetate, and micrographs were recorded on a JEOL JSM-1200EXII electron microscope with an acceleration voltage of 80 kV.

Isothermal Titration Calorimetry. Isothermal titration calorimetry (ITC) was performed at 37 °C on a VP-ITC microcalorimeter (MicroCal iTC200) to measure enthalpies associated with interactions between TA and R3 and between GA and R3. The solution in the syringe had concentrations of 3 mM TA and 30 mM GA. The R3 solution in the 200 μL sample cell was adjusted to a concentration of 0.3 mM. Both solutions were prepared in 50 mM Tris-HCl buffer (pH 7.5) and were degassed before being used. The first drop was set to 0.4 μL, and then the TA solution was titrated into the sample cell as a sequence of 25 injections of 1.6 μL aliquots. The interval between each injection was set as 120 s to achieve complete equilibration. The cell stirring speed was 300 rpm throughout the experiment. A control experiment was performed by titrating TA and GA to buffer, and the resulting reference signal was subtracted from corresponding experimental data. Raw data were obtained as a plot of heating rate (microcalories per second) versus titration time (minutes). Baseline correction and integration of the calorimeter response were conducted using the Origin software provided with the calorimeter. Thermodynamic parameters N (stoichiometry), K_a (association constant), and ΔH (change in enthalpy) were obtained by nonlinear least-squares fitting of experimental data using a single-site binding model of Origin version 7.0 provided with the instrument. The free energy of binding (ΔG) and change in entropy (ΔS) can be calculated using eqs 1 and 2

$$\Delta G = -RT \ln K_a \quad (1)$$

$$\Delta G = \Delta H - T\Delta S \quad (2)$$

where R is the gas constant and T is the temperature in kelvin. The binding affinity of tannic acid for the R3 peptide is given as the dissociation constant ($K_d = 1/K_a$).

Molecular Docking. The structural model of the R3 peptide was constructed by homology modeling using Discovery Studio version 2.5 (Accelrys Inc., San Diego, CA) with template proteins (Protein Data Bank entries 3FQP and 3BKJ) according to a literature method.[29] The three-dimensional structure of tannic acid was obtained through a Gauss View program, and geometry optimization was performed using

dx.doi.org/10.1021/bi400240c | *Biochemistry* 2013, 52, 1893−1902

Gaussian 03.[30] The tannic acid molecule was docked into the R3 peptide through a standard docking procedure using Autodock vina.[31] During the docking process, the TA molecule was regarded as rotatable and subjected to energy minimization. The TA molecule with the optimal orientation was docked into the R3 domain, and the results were imported into Discovery Studio version 2.5 for further rendering.

RESULTS AND DISCUSSION

Inhibition of TA on R3 Aggregation Monitored by ThS Fluorescence. The inhibitory effects of tannic acid and gallic acid on the aggregation of the R3 peptide were investigated by a ThS fluorescence assay.[32] In these experiments, 15 μM R3 in 50 mM Tris-HCl buffer was induced to aggregate by heparin in the presence of ThS which binds to the resulting aggregates and exhibits a dramatic fluorescence change.[33] As reported earlier, the fluorescence intensity in the black curve increases rapidly in the beginning and saturates in ~60 min, indicating that PHF formation proceeds via the steps of nucleation, extension, and PHF.[34] As shown in Figure 2A, the aggregation started slowly and the amount of resulting aggregates decreased greatly in the presence of TA, indicating that tannic acid strongly inhibited R3 assembly. However, gallic acid exhibited a dramatic difference in its ability to inhibit the aggregation of R3. It was merely able to inhibit R3 aggregation, even at relatively high concentrations (Figure 2B). To gain insight into the inhibition mechanism of TA on R3 aggregation, we also independently investigated the inhibitory effects of TA toward the R3 peptide at different stages of aggregation. As shown in Figure 3, the heparin-induced aggregates of the R3 peptide

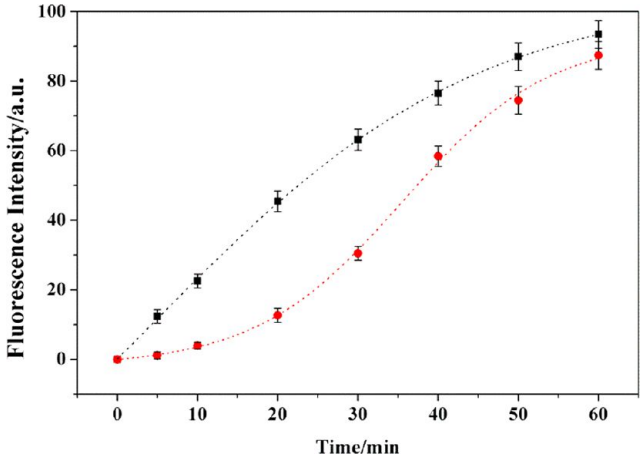

Figure 3. Oligomerization of the R3 peptide (15 μM) in the presence of 3.8 μM heparin and 10 μM ThS. The samples were incubated for 5, 10, 20, 30, 40, 50, and 60 min at 37 °C (■), and then 15 μM TA was added to each sample and the mixture incubated for an additional 2 h (●).

increased quickly as the incubation time gradually extended in the absence of tannic acid. Interestingly, after addition of TA and further incubation, the levels of aggregates decreased to various degrees: a remarkable disaggregation effect was observed during the early stage (0−30 min, corresponding to the nucleation step), while only moderate disaggregation behavior was observed during the later stage (30−60 min, corresponding to the extension step). These results indicate that tannic acid probably can disaggregate the early intermediates such as oligomers that are more critical species than mature fibrils in the tau aggregation process as reported recently.[8,10] This also reveals that TA mainly interacts with the R3 peptide in the nucleation step, not in the extension step.

Again on the basis of the fluorescence change of the aggregate-specific stain ThS as the readout, we performed a R3 aggregation assay in vitro to determine the IC_{50} values of GA and TA, corresponding to the half-maximal inhibitory concentration necessary for their inhibition of R3 assembly into aggregates, as illustrated in Figure 4. A strong inhibitory effect on tau filament assembly (IC_{50} values of 3.5 μM) was observed with TA. Weak inhibition (IC_{50} value of 92 μM) was observed with GA. This IC_{50} sequence is totally in agreement with the result described in the preceding section.

Characterization of the Morphology of the R3 Filament by Electron Microscopy. To confirm the inhibitory effects of TA on R3 aggregation, the resulting filaments assembled in the absence and presence of tannic acid were further examined by electron microscopy. Figure 5 demonstrates the R3 (15 μM) filament morphology assembled under three different conditions: (a) induced independently by heparin, (b) induced by heparin in the presence of 3 μM TA, and (c) induced by heparin in the presence of 15 μM TA. In the absence of TA, the resulting R3 filament was thick and long (~37 nm in width and ~1.9 μm in length) and densely scattered in the solution (Figure 5A). However, in the presence of 3 μM TA, the fibrils became short and thin (~26 nm in width and ~1.1 μm in length) and sparsely populated in the solution (Figure 5B). When the concentration of TA reached 15 μM, only a minute quantity of filaments (~24 nm in width and ~0.5 μm in length) was observed (Figure 5C). The inhibitory effect became more pronounced as the concentration of TA increased. This is consistent with the results of ThS fluorescence experiments; the inhibition of TA on R3 aggregation is dose-dependent.

Thermodynamics of Binding of TA and GA to R3. To evaluate the affinity of TA and GA for tau protein, isothermal titration calorimetry (ITC) experiments were conducted. A typical ITC titration experiment is shown in Figure 6A. The negative peaks of the raw data indicate an exothermic interaction. The binding isotherm is characterized by strong heat release, the amount of which decreases with the titration of TA, until the binding sites on R3 become saturated; in this situation, only dilution heat effects are observed. The stoichiometry (n), association constant (K_a), and change in enthalpy (ΔH) were obtained by nonlinear least-squares fitting of experimental data. The binding of TA to R3 is characterized by a K_a of $(3.64 \pm 0.61) \times 10^4$ M^{-1}, a ΔH of -11.6 ± 0.6 kcal/mol, and an n of 1.02 ± 0.04. Using eq 2 (Materials and Methods), the reaction free energy (ΔG) and entropy (ΔS) were calculated to be −6.47 kcal/mol and −16.6 cal mol^{-1} K^{-1}, respectively. Clearly, the ITC results show a significant recognition of TA for peptide R3.

Figure 6B shows the effects of heat on the binding of GA to R3. Clearly, the binding isotherm of GA is different from that of TA. No notable heat release, but the signal of dilution heat effects, was observed during the titration. It seems that there is only a slight amount of or even no binding between GA and R3. However, we cannot exclude the possibility that an interaction between GA and R3 exists only on the basis of these ITC data, because the interaction between GA and R3 could be in the form of weak hydrogen bonding. In aqueous solution, hydrogen bonding interactions between R3 and water molecules have probably existed. Thus, the net effect of

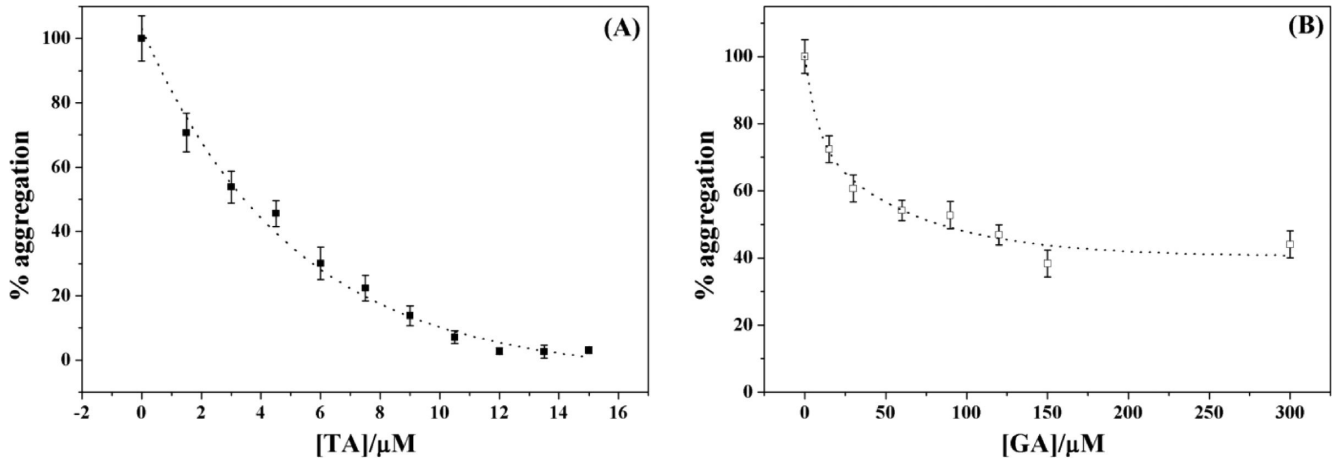

Figure 4. Dose-dependent inhibition of R3 aggregation by tannic acid (A) and gallic acid (B) in 50 mM Tris-HCl buffer (pH 7.5). The concentrations of TA and GA were 0−15 and 0−300 μM, respectively.

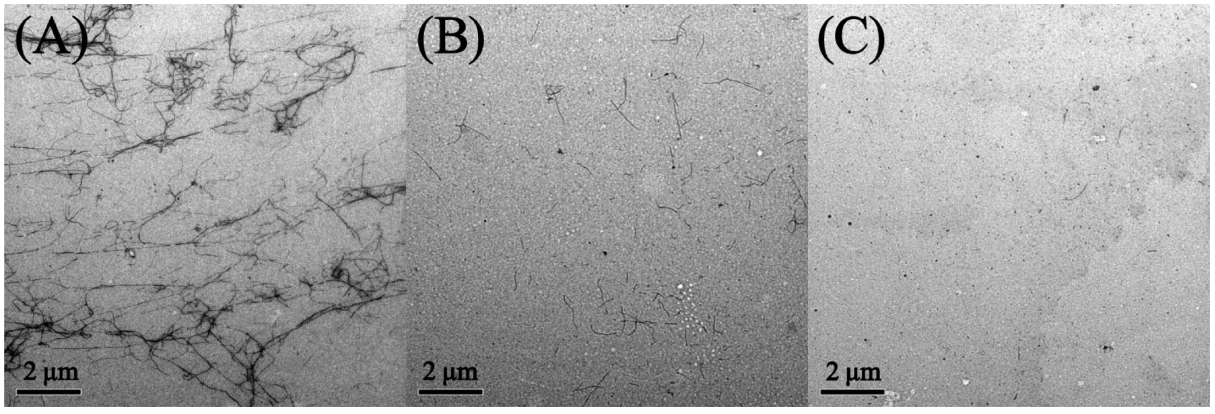

Figure 5. Electron micrographs of aggregated R3 (15 μM). (A) Aggregation induced by heparin (without TA). (B) Aggregation induced by heparin in the presence of 3 μM TA. (C) Aggregation induced by heparin in the presence of equimolar TA (15 μM).

binding of GA to R3 is most likely to be the replacement of hydrogen bonds between water and R3 by newly formed hydrogen bonds between GA and R3. In this process, the energy change should be very small, or even negligible.

Change in the Conformation of R3 Monitored by Its CD Spectrum. The previous methods, such as ThS fluorescence and electron microscopy, can provide only the information about filament formation of tau peptide. The CD spectrum, however, can give us more detailed information about the conformational transition of protein molecules, which is widely believed to be the essential event in the aggregation mechanism. Therefore, the inhibition of aggregation should be closely related to the suppression of the conformational transition.

The impacts of TA on the R3 conformational transition during the aggregation reaction were examined via the CD spectrum. Time-dependent CD spectra recorded during the aggregation process were recorded under two different solution conditions: (a) 15 μM R3 mixed with 3.8 μM heparin in 20 mM phosphate buffer and (b) 15 μM R3 mixed with 3.8 μM heparin and 15 μM TA in 20 mM phosphate buffer (as demonstrated in panels A and B of Figure 7, respectively). TA dose-dependent CD spectra of R3 aggregates are also shown in Figure 7C.

In Figure 7A, we observed how the R3 CD spectrum changed as the aggregation took place in the absence of TA. It is very clear that the magnitude of the strong negative peak at 200 nm gradually decreased, accompanied by the emergence of a negative peak at 216 nm. According to the literature, in the CD spectrum, the positive peak at ∼195 nm and the strong negative peak at 216 nm are usually attributed to typical β-sheet structure, while the strong negative signal near 200 nm is usually attributed to random coil structure.[35,36] Therefore, this profile of the time-dependent CD spectrum indicated that the R3 gradually lost its native random coil structure, with the increase in the level of the β-sheet conformation, as the aggregation advanced in the absence of TA. This result was consistent with the result reported previously.[37]

As illustrated in Figure 7B, in the presence of TA (equimolar), however, no notable CD spectral change was observed even after incubation for ∼38 h, because heparin, the aggregation inducer, was introduced into the mixture, implying that the conformational transition did not occur. In other words, the conformational transition was suppressed by TA, under this condition. Furthermore, in Figure 7C, we noticed that the suppression of the R3 conformational transition by TA exhibited a dose-dependent effect. The higher the concentration of TA, the less obvious the CD spectral change. When the molar ratio of TA to R3 reached 1:1, the predominant conformation of R3 in the incubated mixture was still random coil, the same as that of nonaggregated tau. In other words, the

dx.doi.org/10.1021/bi400240c | *Biochemistry* 2013, 52, 1893−1902

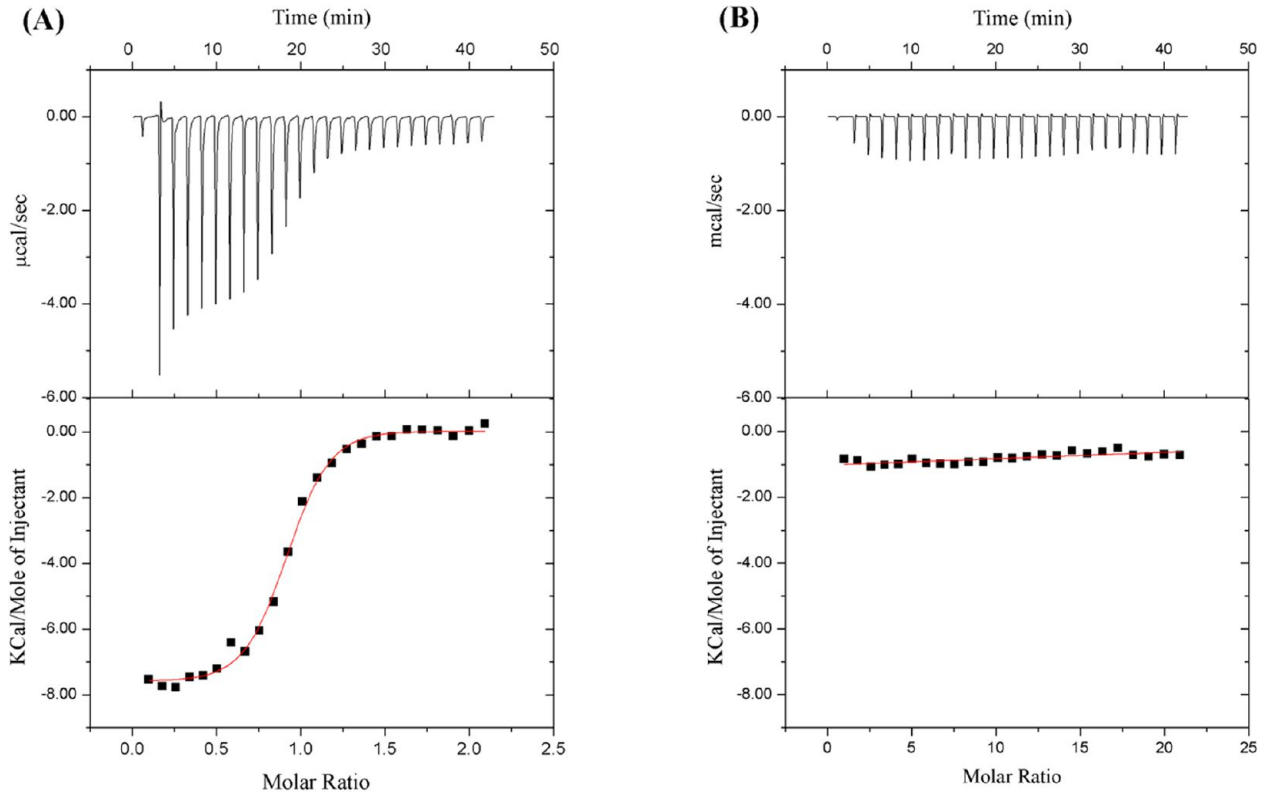

Figure 6. Experimental calorimetric data for the binding of TA and GA to R3. The top panels show the raw data (thermal power). Time integration of the thermal power yields the heat of injection, which is plotted vs the molar ratio of inhibitors to peptide in the bottom panels. The solid lines in the bottom panels represent the least-squares fitting of the data to a one-site binding model. (A) ITC profiles of titration of 3 mM TA to 0.3 mM R3. (B) ITC profiles of titration of 30 mM GA to 0.3 mM R3.

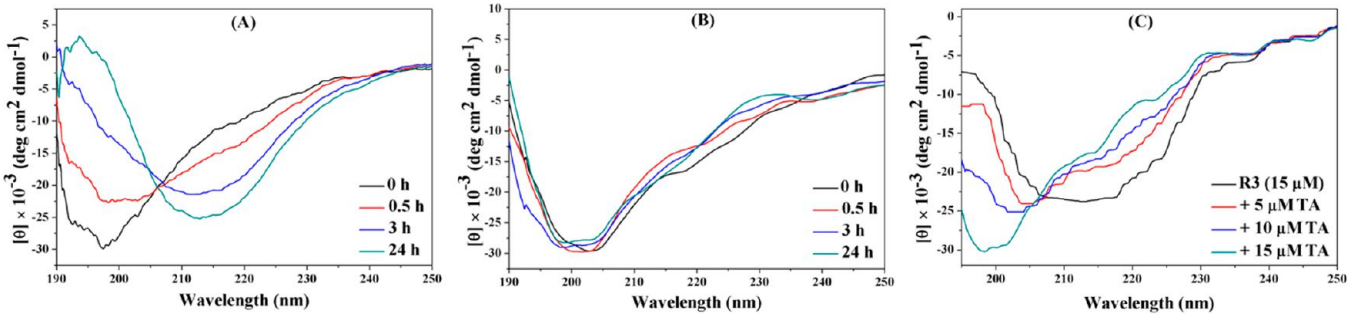

Figure 7. CD spectra of the R3 peptide. (A) Time−CD spectral change profiles of R3 in the presence of heparin alone. (B) Time−CD spectral change profiles of R3 in the presence of heparin and TA. (C) Dose-dependent conformational transition monitored by CD. The reaction mixtures were incubated at 37 °C for 4 h.

conformational transition was almost completely suppressed by TA.

As a control, we also examined the impact of GA on the R3 CD spectrum within the aggregation incubation process. However, we could not observe any different pattern in the CD spectrum that resulted from GA, as the aggregation inhibitor (data not shown), indicating the conformational transition of R3 could not be suppressed by GA.

Molecular Docking. On the basis of the experimental studies described above, a molecular docking simulation of tannic acid with the R3 peptide was performed using Autodock vina.[31] The R3 monomer was constructed according to a literature method[38] with minor variations. During the docking process, the TA molecule was regarded as rotatable and subjected to energy minimization. The docking result with the optimal orientation is shown in Figure 8. The binding affinity in this model was calculated as −9.7 kcal/mol. The surface model in Figure 9 showed that the TA molecule was docked into the hydrophobic cave of R3, which indicates the existence of hydrophobic interactions. In a word, the binding between TA and R3 is characterized by essential hydrophobic interactions and plenty of hydrogen bonding interactions.

The binding orientations from the hypothesized binding model of TA on R3 (Figure 8) are as follows. (i) Three of the outside aromatic rings (A, B, and D) in TA are located in the β-sheet region of the N-terminus of R3 (^{306}VQIVYK^{311}). (ii) The other two outside aromatic rings (C and E) are located in the middle of the R3 peptide. (iii) All the inside aromatic rings gather around the center of the binding pocket. (iv) The aromatic rings outside each form one or two hydrogen bonds

dx.doi.org/10.1021/bi400240c | *Biochemistry* 2013, 52, 1893−1902

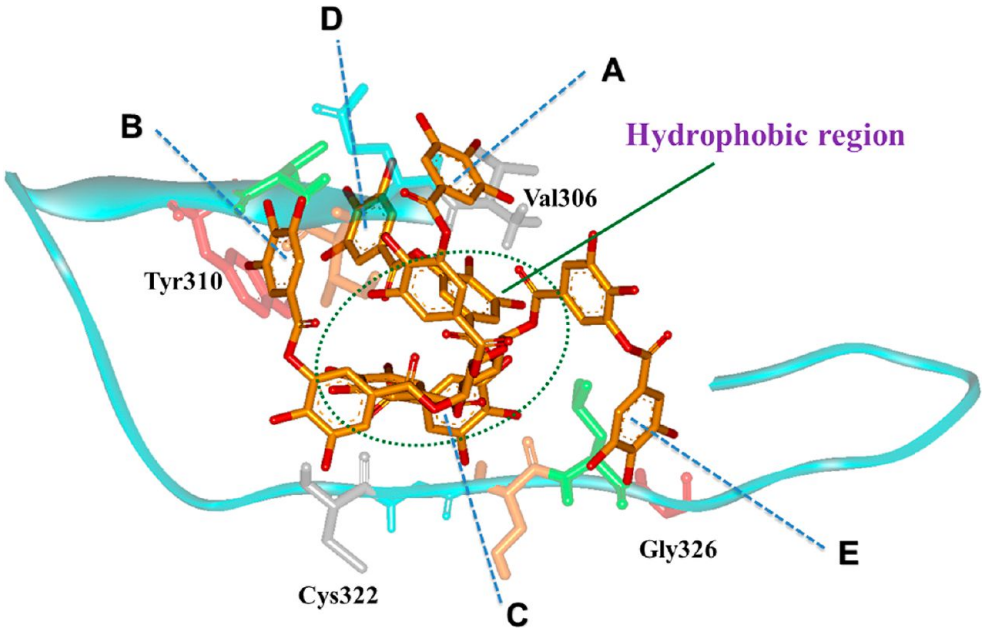

Figure 8. Binding of tannic acid to the R3 peptide. The hydrophobic region is marked with a green dotted oval.

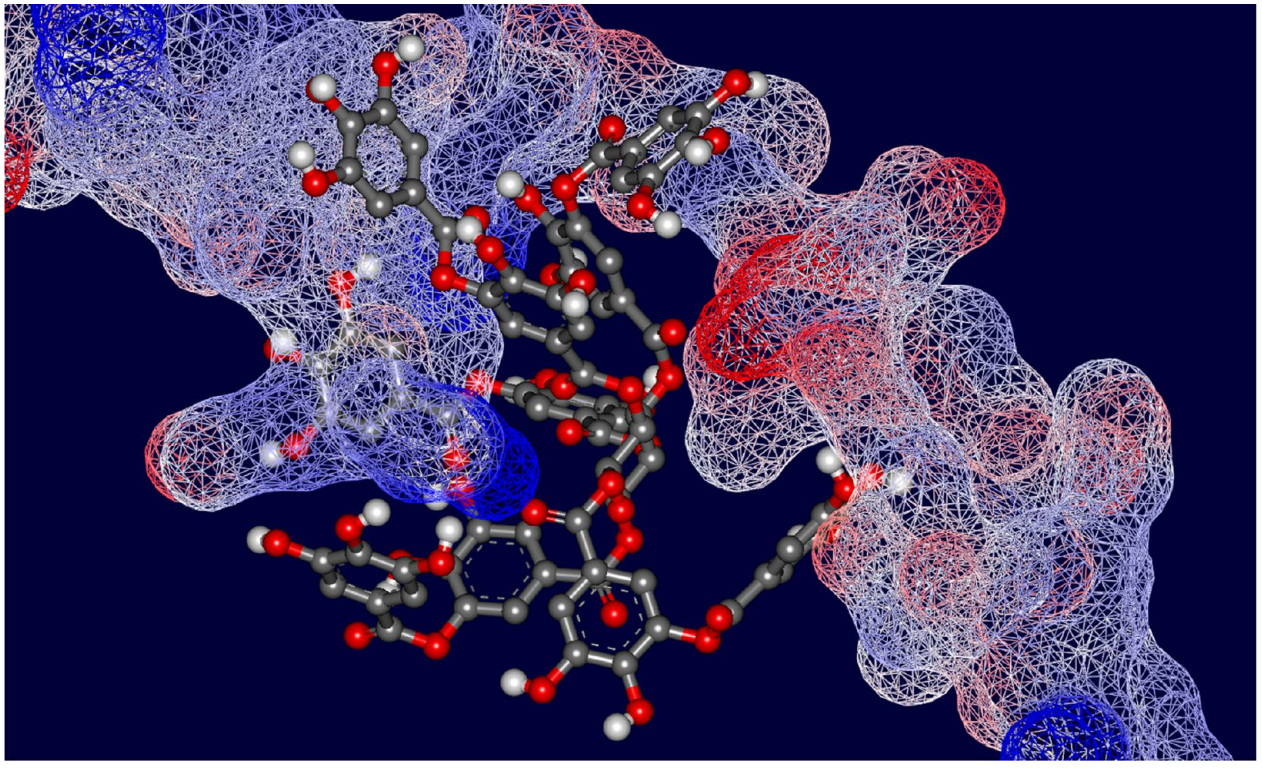

Figure 9. Molecular surface of the R3 peptide colored by interpolated charge.

with the residues or the main chain of R3, and the inside aromatic rings and central glucose ring may interact with R3 through hydrophobic interactions. Both hydrogen bonding and hydrophobic interactions may play an essential part in the inhibition of tau aggregation by inhibitors. The hydrogen bonds between R3 and tannic acid are probably formed between (i) hydroxyl groups of TA at aromatic ring A and the backbone amide hydrogen and carbonyl oxygen of Val306 and the side chain carbonyl oxygen of Gln307, (ii) hydroxyl groups of TA at aromatic ring B and the backbone amide hydrogen and carbonyl oxygen of Ile308 and the backbone amide hydrogen of Val309, (iii) hydroxyl groups of TA at aromatic ring C and the backbone amide hydrogen and carbonyl oxygen of Ser324, (iv) hydroxyl groups of TA at aromatic ring D and the side chain phenolichydroxyl oxygen of Tyr310, and (v) hydroxyl groups of TA at aromatic ring E and the backbone carbonyl oxygen of Gly326 and the backbone amide hydrogen of Leu325. The hydrophobic region of R3 that contributes to the hydrophobic interaction between tannic acid and R3 may be formed by the

dx.doi.org/10.1021/bi400240c | *Biochemistry* 2013, 52, 1893−1902

combination of Val306, Gln307, Ile308, Val309, Tyr310, Lys321, Cys322, Gly323, Ser324, Leu325, and Gly326.

Model of R3 Aggregation and Inhibition. The R3 peptide is potentially the most important repeat to act as a trigger to initiate the molecular aggregation of full tau protein. The ^{306}VQIVYK^{311} amino acid sequence, located in the N-terminal region of R3, has been proven to adopt a β-sheet conformation upon aggregation and has been shown to be the core structural elements for filament elongation.[28] One of the common features of the ^{306}VQIVYK^{311} sequence is edge-to-edge hydrogen bonding interaction within the parallel β-sheet. This β-sheet has a somewhat amphipathic nature, with several hydrophobic residues on one face, with a relatively polar face opposite. In this situation, the amphipathic strands would form horizontal sheets that could then stack on top of one another to propagate filament growth. Simultaneously, the remainder of the peptide chain behind the ^{306}VQIVYK^{311} sequence is aligned together and forms highly ordered structures, for example, α-helix, in the middle region of R3. Interactions among the resulting ordered structures would be another driving force for tau aggregation. The model of R3 polymerization and growth is illustrated in Figure 10 A with a cartoon.

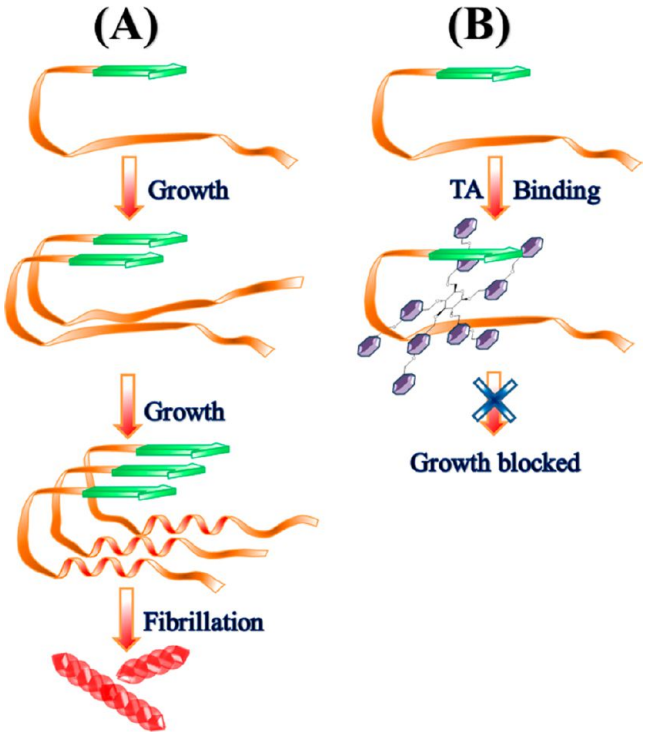

Figure 10. Parallel-growth model of the R3 peptide (A) and inhibition of parallel growth by tannic acid (B).

On the basis of the experimental results and the docking results, we proposed a model to provide insight into the inhibition mechanism of R3 aggregation by TA, the molecular inhibitor, as illustrated in Figure 10 B. As shown in this model, tannic acid is assumed to intercalate into the hydrophobic cave of the R3 peptide. The TA molecule holds the peptide chain of R3 probably at two positions, one at the N-terminus and another at the middle of the peptide chain. Filament growth is blocked by at least two factors. First, chelated by the TA molecule, the peptide chain of R3 is refolded like a hairpin. This hairpin folding motif greatly reduced the flexibility of peptide R3, resulting in a negative entropy change and a stabilization in random coil structure, as we observed in the ITC and CD experiments, respectively. Second, the hydrogen bonding edge of the ^{306}VQIVYK^{311} sequence and the hydrophobic region in the center of the peptide chain are both capped by the tannic acid molecule, preventing the formation of β-sheet structure and the further alignment of the rest of the peptide chain.

As for GA, although it could be regarded as the molecular monomer of TA, its molecule contains the same aromatic ring and phenol group; however, no central glucose ring exists, and the aromatic rings and phenol groups in GA are not specially oriented by the central glucose ring as in the TA molecule. Therefore, the shape and/or size of the GA molecule does not fit in the hydrophobic cave of the R3 peptide. The GA molecule cannot dock into the hydrophobic cave of R3 to form such a hairpin structure, because of the lack of the central glucose ring, and special arrangement of aromatic rings and phenol groups. There is no molecular recognition or targeting of binding between GA and R3 because of the inappropriate molecular size and group orientation.

Inhibition by TA of Human Full-Length Tau Protein. We have demonstrated that TA competently inhibits the in vitro aggregation of R3, a key fragment of tau protein, implying the possibility of TA as a leading compound of anti-AD drugs. These results aroused our interest and raised the question of TA's inhibition of human full-length tau. This question is even more important to drug discovery, although the investigation should be difficult because of the complexity of full-length tau interacting with the TA molecule. However, the data and the proposed model in our previous discussion have established a solid foundation for our subsequent studies. In this paper, we would like to have a preliminary test; electron microscopy was manipulated for a semiquantitative assessment of filament formation of human full-length tau protein, in the absence or presence of TA in solution. The experimental process is described in Materials and Methods. Figure 11 shows the full-length tau filament morphology assembled under three different conditions: (a) induced independently by heparin, (b) induced by heparin in the presence of 30 μM TA, and (c) induced by heparin in the presence of 60 μM TA. Excitingly, the aggregation of full-length tau was found to be effectively inhibited by tannic acid. In the absence of TA, the resulting filaments densely scattered in the solution; in the presence of 30 μM TA, the sparsely populated fibrils became short and thin, and when the concentration of TA reached 60 μM, filaments were barely observed. These results confirmed the potential of tannic acid as a drug candidate.

Finally, we have to note that the TA molecule is highly polar and probably difficult for it to penetrate the blood–brain barrier directly. However, there are many fully developed drug carriers, such as liposomes and nanoparticles, that can overcome this barrier and successfully transport drugs into the brain.[39−42] Therefore, compounds with a low membrane permeability but a strong inhibitory effect are also promising molecules with the help of drug delivery technologies.

■ CONCLUSION

The identification of aggregation inhibitors and the investigation of their binding mode are important steps in addressing fundamental issues for the design of anti-AD drugs and the screening of compound libraries. At present, enhancing the targeting and efficacy of the aggregation inhibitor at the SAR (structure–activity relationship) level is the main strategy in the

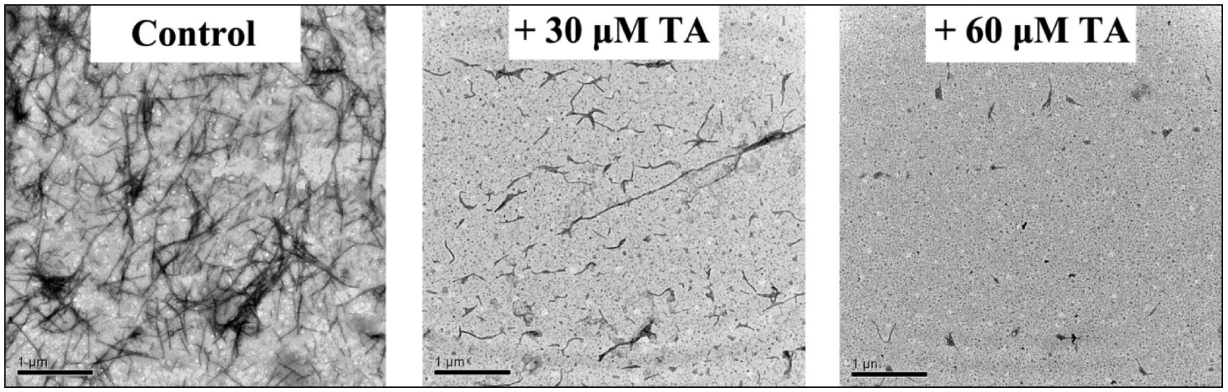

Figure 11. Electron microscopic analysis of full-length tau filaments incubated in the absence (Control) or presence of tannic acid (30 and 60 μM).

development of the next generation of small-molecule inhibitors. Inspired by the success in inhibiting the aggregation of Aβ,[24,25] we performed, for the first time, multiple experiments to elucidate the binding properties and aggregation inhibitory activity of tannic acid, a plant polyphenol, on tau peptide R3, in comparison with its moiety, gallic acid (GA).

We found that TA shows significant affinity for tau peptide R3, while its monomer, GA, does not. The strong binding of TA to R3 can suppress the conformational transition in filament formation and, hence, break the tau−tau interaction and inhibit the self-aggregation of R3. With regard to the structural difference between TA and GA, the recognition of TA toward R3 may be dominated by hydrophobic interactions by the central glucose ring and adjacent aromatic rings, in addition to hydrogen bonds. In addition, the strong affinity of TA for R3 may be also closely related to specific structural features: hydrophobic center, appropriate size, and numerous phenol groups. Furthermore, our researches interestingly suggest that the recognition by TA of tau peptide R3 may depend on the formation of a hairpin structure, a key structural feature required for inhibiting tau polymerization, in addition to hydrogen bonds, hydrophilic−hydrophobic interactions, and static electrical interactions, as reported earlier.

The results obtained may be useful for elucidating the inhibition mechanism of PHF formation in Alzheimer's disease and offering a new stratagem for the rational molecular design of tau aggregation inhibitors.

AUTHOR INFORMATION

Corresponding Author

*Telephone: +86 21 65983292. Fax: +86 21 65983292. E-mail: tmyao@tongji.edu.cn (T.Y.) or shishuo@tongji.edu.cn (S.S.).

Funding

This work was supported by the National Science of Foundation of China (81171646, 20871094, 31170776, and 20901060) and the Fundamental Research Funds for the Central Universities.

Notes

The authors declare no competing financial interest.

ABBREVIATIONS

AD, Alzheimer's disease; TA, tannic acid; GA, gallic acid; MBD, microtubule-binding domain; R3, third repeat of MBD; NFTs, neurofibrillary tangles; SPs, senile plaques; PHFs, paired helical filaments; SAR, structure−activity relationship; IC_{50}, half-maximal inhibitory concentration.

REFERENCES

(1) Selkoe, D. J., and Schenk, D. (2003) Alzheimer's Disease: Molecular Understanding Predicts Amyloid-Based Therapeutics. *Annu. Rev. Pharmacol. 43*, 545−584.

(2) Mandelkow, E.-M., and Mandelkow, E. (1998) Tau in Alzheimer's disease. *Trends Cell Biol. 8*, 425−427.

(3) Lee, V. M.-Y., Goedert, M., and Trojanowski, J. Q. (2001) Neurodegenerative Tauopathies. *Annu. Rev. Neurosci. 24*, 1121−1159.

(4) Iqbal, K., Liu, F., Gong, C.-X., Alonso, A., and Grundke-Iqbal, I. (2009) Mechanisms of tau-induced neurodegeneration. *Acta Neuropathol. 118*, 53−69.

(5) Inouye, H., Sharma, D., Goux, W. J., and Kirschner, D. A. (2006) Structure of Core Domain of Fibril-Forming PHF/Tau Fragments. *Biophys. J. 90*, 1774−1789.

(6) Arriagada, P. V., Growdon, J. H., Hedley-Whyte, E. T., and Hyman, B. T. (1992) Neurofibrillary tangles but not senile plaques parallel duration and severity of Alzheimer's disease. *Neurology 42*, 631.

(7) Iqbal, K., del C. Alonso, A., Chen, S., Chohan, M. O., El-Akkad, E., Gong, C.-X., Khatoon, S., Li, B., Liu, F., Rahman, A., Tanimukai, H., and Grundke-Iqbal, I. (2005) Tau pathology in Alzheimer disease and other tauopathies. *Biochim. Biophys. Acta 1739*, 198−210.

(8) Meraz-Ríos, M. A., Lira-De León, K. I., Campos-Peña, V., De Anda-Hernández, M. A., and Mena-López, R. (2010) Tau oligomers and aggregation in Alzheimer's disease. *J. Neurochem. 112*, 1353−1367.

(9) Berger, Z., Roder, H., Hanna, A., Carlson, A., Rangachari, V., Yue, M., Wszolek, Z., Ashe, K., Knight, J., Dickson, D., Andorfer, C., Rosenberry, T. L., Lewis, J., Hutton, M., and Janus, C. (2007) Accumulation of Pathological Tau Species and Memory Loss in a Conditional Model of Tauopathy. *J. Neurosci. 27*, 3650−3662.

(10) Maeda, S., Sahara, N., Saito, Y., Murayama, M., Yoshiike, Y., Kim, H., Miyasaka, T., Murayama, S., Ikai, A., and Takashima, A. (2007) Granular Tau Oligomers as Intermediates of Tau Filaments. *Biochemistry 46*, 3856−3861.

(11) Bulic, B., Pickhardt, M., Khlistunova, I., Biernat, J., Mandelkow, E.-M., Mandelkow, E., and Waldmann, H. (2007) Rhodanine-Based Tau Aggregation Inhibitors in Cell Models of Tauopathy. *Angew. Chem., Int. Ed. 46*, 9215−9219.

(12) Khlistunova, I., Pickhardt, M., Biernat, J., Wang, Y., Mandelkow, E.-M., and Mandelkow, E. (2007) Inhibition of Tau Aggregation in Cell Models of Tauopathy. *Curr. Alzheimer Res. 4*, 544−546.

(13) Gregor, L., Marcus, P., David, G. L., Boris, S., and Eckhard, M. (2007) Screening for Inhibitors of Tau Protein Aggregation into Alzheimer Paired Helical Filaments: A Ligand Based Approach Results in Successful Scaffold Hopping. *Curr. Alzheimer Res. 4*, 315−323.

(14) Pickhardt, M., Bergen, M. v., Gazova, Z., Hascher, A., Biernat, J., Mandelkow, E.-M., and Mandelkow, E. (2005) Screening for Inhibitors of Tau Polymerization. *Curr. Alzheimer Res. 2*, 219−226.

(15) Pickhardt, M., Biernat, J., Khlistunova, I., Wang, Y. P., Gazova, Z., Mandelkow, E. M., and Mandelkow, E. (2007) N-Phenylamine Derivatives as Aggregation Inhibitors in Cell Models of Tauopathy. *Curr. Alzheimer Res. 4*, 397−402.

(16) Bulic, B., Pickhardt, M., Mandelkow, E.-M., and Mandelkow, E. (2010) Tau protein and tau aggregation inhibitors. *Neuropharmacology 59*, 276−289.
(17) Brunden, K. R., Ballatore, C., Crowe, A., Smith, A. B., III, Lee, V. M., and Trojanowski, J. Q. (2010) Tau-directed drug discovery for Alzheimer's disease and related tauopathies: A focus on tau assembly inhibitors. *Exp. Neurol. 223*, 304−310.
(18) Bulic, B., Pickhardt, M., Schmidt, B., Mandelkow, E.-M., Waldmann, H., and Mandelkow, E. (2009) Development of Tau Aggregation Inhibitors for Alzheimer's Disease. *Angew. Chem., Int. Ed. 48*, 1740−1752.
(19) Chang, E., Congdon, E. E., Honson, N. S., Duff, K. E., and Kuret, J. (2009) Structure−Activity Relationship of Cyanine Tau Aggregation Inhibitors. *J. Med. Chem. 52*, 3539−3547.
(20) Zheng, J., Liu, C., Sawaya, M. R., Vadla, B., Khan, S., Woods, R. J., Eisenberg, D., Goux, W. J., and Nowick, J. S. (2011) Macrocyclic β-Sheet Peptides That Inhibit the Aggregation of a Tau-Protein-Derived Hexapeptide. *J. Am. Chem. Soc. 133*, 3144−3157.
(21) Taniguchi, S., Suzuki, N., Masuda, M., Hisanaga, S.-i., Iwatsubo, T., Goedert, M., and Hasegawa, M. (2005) Inhibition of Heparin-induced Tau Filament Formation by Phenothiazines, Polyphenols, and Porphyrins. *J. Biol. Chem. 280*, 7614−7623.
(22) Costa, E., Coelho, M., Ilharco, L. M., Aguiar-Ricardo, A., and Hammond, P. T. (2011) Tannic Acid Mediated Suppression of PNIPAAm Microgels Thermoresponsive Behavior. *Macromolecules 44*, 612−621.
(23) Han, L.-J., Shi, S., Zheng, L.-F., Yang, D.-J., Yao, T.-M., and Ji, L.-N. (2010) Flavonoids Inhibit Heparin-Induced Aggregation of the Third Repeat (R3) of Microtubule-Binding Domain of Alzheimer's Tau Protein. *Bull. Chem. Soc. Jpn. 83*, 911−922.
(24) Porat, Y., Abramowitz, A., and Gazit, E. (2006) Inhibition of Amyloid Fibril Formation by Polyphenols: Structural Similarity and Aromatic Interactions as a Common Inhibition Mechanism. *Chem. Biol. Drug Des. 67*, 27−37.
(25) Ono, K., Hasegawa, K., Naiki, H., and Yamada, M. (2004) Anti-amyloidogenic activity of tannic acid and its activity to destabilize Alzheimer's β-amyloid fibrils in vitro. *Biochim. Biophys. Acta 1690*, 193−202.
(26) Tomoo, K., Yao, T.-M., Minoura, K., Hiraoka, S., Sumida, M., Taniguchi, T., and Ishida, T. (2005) Possible Role of Each Repeat Structure of the Microtubule-Binding Domain of the Tau Protein in In Vitro Aggregation. *J. Biochem. 138*, 413−423.
(27) Jiang, L.-F., Yao, T.-M., Zhu, Z.-L., Wang, C., and Ji, L.-N. (2007) Impacts of Cd(II) on the conformation and self-aggregation of Alzheimer's tau fragment corresponding to the third repeat of microtubule-binding domain. *Biochim. Biophys. Acta 1774*, 1414−1421.
(28) von Bergen, M., Friedhoff, P., Biernat, J., Heberle, J., Mandelkow, E.-M., and Mandelkow, E. (2000) Assembly of τ protein into Alzheimer paired helical filaments depends on a local sequence motif (^{306}VQIVYK^{311}) forming β structure. *Proc. Natl. Acad. Sci. U.S.A. 97*, 5129−5134.
(29) Modi, S., Paine, M. J., Sutcliffe, M. J., Lian, L. Y., Primrose, W. U., Wolf, C. R., and Roberts, G. C. K. (1996) A Model for Human Cytochrome P450 2D6 Based on Homology Modeling and NMR Studies of Substrate Binding. *Biochemistry 35*, 4540−4550.
(30) Frisch, M. J., et al. (2005) *Gaussian 03*, revision D.01, Gaussian Inc., Wallingford, CT.
(31) Trott, O., and Olson, A. J. (2010) AutoDock Vina: Improving the speed and accuracy of docking with a new scoring function, efficient optimization, and multithreading. *J. Comput. Chem. 31*, 455−461.
(32) Goux, W. J., Kopplin, L., Nguyen, A. D., Leak, K., Rutkofsky, M., Shanmuganandam, V. D., Sharma, D., Inouye, H., and Kirschner, D. A. (2004) The Formation of Straight and Twisted Filaments from Short Tau Peptides. *J. Biol. Chem. 279*, 26868−26875.
(33) Friedhoff, P., Schneider, A., Mandelkow, E.-M., and Mandelkow, E. (1998) Rapid Assembly of Alzheimer-like Paired Helical Filaments from Microtubule-Associated Protein Tau Monitored by Fluorescence in Solution. *Biochemistry 37*, 10223−10230.
(34) Friedhoff, P., von Bergen, M., Mandelkow, E.-M., Davies, P., and Mandelkow, E. (1998) A nucleated assembly mechanism of Alzheimer paired helical filaments. *Proc. Natl. Acad. Sci. U.S.A. 95*, 15712−15717.
(35) von Bergen, M., Barghorn, S., Biernat, J., Mandelkow, E.-M., and Mandelkow, E. (2005) Tau aggregation is driven by a transition from random coil to β sheet structure. *Biochim. Biophys. Acta 1739*, 158−166.
(36) Minoura, K., Yao, T.-M., Tomoo, K., Sumida, M., Sasaki, M., Taniguchi, T., and Ishida, T. (2004) Different associational and conformational behaviors between the second and third repeat fragments in the tau microtubule-binding domain. *Eur. J. Biochem. 271*, 545−552.
(37) Mizushima, F., Minoura, K., Tomoo, K., Sumida, M., Taniguchi, T., and Ishida, T. (2006) Fluorescence-coupled CD conformational monitoring of filament formation of tau microtubule-binding repeat domain. *Biochem. Biophys. Res. Commun. 343*, 712−718.
(38) Miller, Y., Ma, B., and Nussinov, R. (2011) Synergistic Interactions between Repeats in Tau Protein and Aβ Amyloids May Be Responsible for Accelerated Aggregation via Polymorphic States. *Biochemistry 50*, 5172−5181.
(39) Kabanov, A. V., and Batrakova, E. V. (2004) New Technologies for Drug Delivery across the Blood Brain Barrier. *Curr. Pharm. Des. 10*, 1355−1363.
(40) Tucker, I. G., Yang, L., and Mujoo, H. (2012) Delivery of drugs to the brain via the blood brain barrier using colloidal carriers. *J. Microencapsulation 29*, 475−486.
(41) Kreuter, J. (2012) Nanoparticulate systems for brain delivery of drugs. *Adv. Drug Delivery Rev. 64* (Suppl.), 213−222.
(42) Hossaina, S., Akaike, T., and Chowdhury, E. H. (2010) Current Approaches for Drug Delivery to Central Nervous System. *Curr. Drug Delivery 7*, 389−397.